UCRL-95670

Preprint

UCRL--95670

DE87 012628

Experimental Characteristics of a High-Gain Free-Electron Laser Amplifier Operating at 8-mm and 2-mm Wavelengths

A. L. Throop, T. J. Orzechowski,
B. R. Anderson, F. W. Chambers,
J. C. Clark, W. M. Fawley, R. A. Jong,
A. C. Paul, D. Prosnitz,
E. T. Scharlemann, R. D. Stever,
G. A. Westenskow, and S. M. Yarema
Lawrence Livermore National Laboratory

K. Halbach, D. B. Hopkins,
and A. M. Sessler
Lawrence Berkeley Laboratory

Prepared for AIAA 19th Fluid Dynamics,
Plasma Dynamics, and Laser Conference
Honolulu, Hawaii
June 8-10, 1987

Beam Research Program

Lawrence Livermore National Laboratory

EXPERIMENTAL CHARACTERISTICS OF A HIGH-GAIN FREE-ELECTRON LASER AMPLIFIER OPERATING AT 8-MM AND 2-MM WAVELENGTHS

A. L. Throop, T. J. Orzechowski, B. R. Anderson, F. W. Chambers, J. C. Clark, W. M. Fawley, R. A. Jong, A. C. Paul, D. Prosnitz, E. T. Scharlemann, R. D. Stever, G. A. Westenskow, and S. M. Yarema

Lawrence Livermore National Laboratory*
Livermore, California

K. Halbach, D. B. Hopkins, and A. M. Sessler

Lawrence Berkeley Laboratory†
Berkeley, California

June 8, 1987

ABSTRACT

The Electron Laser Facility (ELF) at the Lawrence Livermore National Laboratory (LLNL) uses a high-current induction linac (3.5 MeV, 1000 A), in conjunction with a pulsed electromagnetic wiggler (4.0 m, 4000 G), to operate a free electron laser (FEL) that produces intense radiation in the microwave regime (2-8 mm). ELF is a high-gain, single-pass amplifier, using a commercial microwave source as an oscillator input (200 W-50 kW). Previous experiments at 35 GHz produced exponential gains of 40 dB/m, peak powers exceeding 1 GW, and beam-to-RF conversion efficiencies of 34%. Recent experiments at 140 GHz have demonstrated exponential gains of 22 dB/m, peak powers exceeding 50 MW, and total gains of 65 dB. In this paper, we describe the experimental results at these two frequencies and compare them with the predictions of simulation codes.

*Performed under the auspices of the U.S. Department of Energy by LLNL under W-7405-ENG-48 and for the Department of Defense under SDIO/BMD/ATC MIPR No. W3-RDP-A127.

†Supported by the Director, Advanced Energy Sciences, Office of Energy Research, U. S. Department of Energy, under Contract No. DE-AC03-76SF00098.

INTRODUCTION

The ELF experiment at LLNL was constructed to study the physics of high-gain FEL amplifiers and has served as a verification for simulation codes. ELF operates in the microwave regime, at frequencies of 35 and 140 GHz; the range is determined primarily by the beam energy of the existing Experimental Test Accelerator (ETA).

Most of the experiments in ELF have been at 35 GHz and have demonstrated high-peak power (1 GW) and conversion efficiency (34%). The high power and conversion efficiency have prompted recent interest in using a microwave FEL to drive a high-gradient RF accelerator in a two-beam accelerator configuration,[2] and for heating and current drive in Tokamaks.[3] In this paper, we review the 35 GHz ELF experiments and report on experiments at 140 GHz that were partly motivated by these interests.

DESCRIPTION OF THE ELF FACILITY

The electron beam for the experiment is provided by the ETA, an induction linear accelerator that can produce a 4.5-MeV, 10-kA, 30-ns electron beam pulse.[4] The parameters of the ETA as used for FEL experiments are summarized in Table 1.

The configuration of the ELF wiggler beamline is shown in Fig. 1. An emittance selector, with a maximum acceptance of 0.4 π rad-cm (normalized), transmits a beam of about 1600 A with a brightness of about 2×10^4 A/(cm-rad)^2. A series of focusing quadrupole and steering dipole magnets is used to match the beam to the input of the wiggler.

Figure 2 shows a photograph of a 1-m section of the ELF wiggler. The external field coils visible in Fig. 1 are quadrupoles (30 G/cm) used to

provide horizontal focusing of the beam in the wiggler. The wiggler is a pulsed electromagnet (1-ms pulse width) comprising a linear array of alternately opposed solenoids, located above and below the interaction region that can be seen at the axis of the wiggler section. When the wiggler is fully assembled, the interaction region contains an oversized (3 x 10 cm) waveguide for colinear propagation of the beam and microwave signals. The fields of the solenoid array combine to form a linearly polarized magnetic field that is purely transverse on axis, and whose amplitude varies sinusoidally with a period of 9.8 cm along the length of the wiggler. The ELF wiggler is nominally 4-m long, consisting of 40 wiggler periods. The current in each two periods of the wiggler can be independently controlled, allowing the strength of the wiggler field to be arbitrarily varied ("tapered") along the length of the wiggler.

The microwave beamline is also shown in Fig. 1. For 35-GHz operation, a magnetron provides about 50-100 kW of peak power over a 500-ns pulse. The power then propagates via an oversized waveguide to a "transition" section where the electron beam and RF signal are combined, colinearly, into the wiggler. The propagation section provides transit-time isolation of the source from reflections of the 15-ns high-power output pulse. A thin (0.0002 in.) electroformed mesh (60 lpi for 35-GHz experiments) reflects the microwave signal into the wiggler waveguide; the electron beam passes through the mesh with no significant degradation. The waveguide inside the wiggler is approximately 3 x 10 cm, made of 0.060-in. stainless-steel walls. Smooth waveguide tapers launch a TE_{01} mode into the waveguide. Measurements of the pulsed wiggler field inside the waveguide show that the effects of eddy currents are negligible.

At the wiggler output, the electron beam is deflected into the waveguide wall. The amplified microwave signal is guided to a diffraction loss chamber that reduces the microwave power to a level that can be handled by conventional microwave components. Waveguide filters ensure the spectral purity of the FEL signal, while calibrated attenuators and crystal detectors are used to measure power levels. Thermistor or thermocouple power meters provide an absolute power reference for calibrating the crystal sensitivity and measuring system attenuation. The attenuation of the microwave beamline from the wiggler output to the detector crystals is determined in two ways--by measuring the overall attenuation (~60 dB) in increments of less than 30 dB using lower-power continuous-wave (CW) sources with a power meter, and by measuring the overall attenuation of the high-power input signal to the crystal detector. The two values obtained in this manner usually agree within 1 dB. Table 1 summarizes the experimental parameters of ELF.

The FRED and GINGER simulation codes[4,5] are used to model the FEL interaction. FRED is a two-dimensional (r,z), monochromatic code that follows the electron energies and phases in the ponderomotive well using the KMR equations,[7] while the fields evolve using the paraxial wave equation. Three-dimensional waveguide modes are modeled by assuming a transverse cosine field variation. FRED also models such effects as finite beam size, velocity distributions, waveguide modes, and longitudinal space charge. GINGER is a time-dependent extension of FRED used to study broadband-spectrum and sideband growth in an FEL.

35-GHZ RESULTS

The condition for FEL synchronism[8] in a waveguide is:

$$2\gamma^2 = \frac{\frac{\omega}{c}(1 + a_w^2)}{[k_w + (k - \frac{\omega}{c})]} \quad , \tag{1}$$

where $\omega^2 = k^2c^2 + \omega_{co}^2$, $k_w = \frac{2\pi}{\lambda_w}$,

$$\frac{\omega_{co}^2}{\pi^2 c^2} = \frac{m^2}{a^2} + \frac{n^2}{b^2} \tag{2}$$

for a TE_{mn} mode, and

$$a_w = \frac{e}{\sqrt{2}mc} \frac{B_w}{k_w} \quad . \tag{3}$$

This expression reduces to the usual free-space expression for $\omega = kc$. For 35-GHz operation of ELF, $a_w \simeq 2.4$, so that $a_w^2 >> 1$. The interaction waveguide has a cutoff frequency of 5.2 GHz, so that dispersive effects are small. Figure 3 plots the synchronism condition [Eq. (1)] for ELF experimental parameters and illustrates the inherent tunability of the FEL source. At 3.5-MeV beam energy and 35-GHz signal frequency, FEL synchronism occurs at a wiggler field strength of 4.5 kG. At 140 GHz, the wiggler field becomes 2.0 kG for synchronism with identical beam conditions. Corrections resulting from emittance, off-axis wiggler field variations, and space charge reduce the actual wiggler field for peak gain from that of Eq. (1).

Figure 4 shows a detuning curve (microwave power vs wiggler field) for a 35-GHz input signal and a 1-m wiggler length, along with simulation results. The curve peaks at a magnetic field of 3.8 kG, with a profile that agrees with simulations. However, the simulations produce a detuning curve that peaks at a magnetic field 7% higher (for 3.5 MeV) than the experimental peak. In the

comparisons between experiment and simulation that follow, we assume operation at the peak of the respective detuning curves.

Figure 5 shows a typical "gain curve" for the FEL interaction over a 3-m constant wiggler. Also shown is the gain curve calculated by simulation for the specific experimental conditions. To produce the gain curve, the length of the FEL interation is reduced by adjusting, in succession, the magnetic field of each two-period wiggler segment to an off-resonance value, and measuring the output power at each setting. Typical growth rates are 35 dB/m, with saturation of the signal at about 1.4 m, followed by synchrotron oscillations as the trapped electrons oscillate in the ponderomotive well.

As shown by the lower trace in Fig. 6, peak conversion efficiencies of about 6% are measured at the onset of saturation. This efficiency can be improved by axially "tapering" the strength of the wiggler field after saturation in order to maintain FEL synchronism.[7,9] Figure 6 compares gain curves measured for a uniform and a tapered wiggler. By proper tapering, we can continue to extract energy from the electron-beam bunches that have been trapped in the ponderomotive well. The output RF power increases by more than a factor of five from that measured at the saturation point, and the conversion efficiency exceeds 35%. As can be seen, these results are in good agreement with FRED simulations. The simulations indicate over 70% of the electrons in the beam are trapped.[10]

Figure 7 illustrates the inherently large frequency range over which the FEL amplifier can operate at a fixed wiggler setting. This is of interest in such applications as control of the disruption instability in Tokamaks, where one wants to vary the FEL frequency rapidly (1-ms timescale) over ±3-5%. Figure 7 shows a detuning curve for a tapered wiggler at 35 GHz. The wiggler

field can be varied by more than 10% without significantly reducing the output power. From Eq. (1), for large a_w, the range over which the frequency of the input signal can be varied (for a fixed wiggler field) is twice that of the magnetic field, corresponding to a frequency bandwidth of about ±10%. Code simulations for higher-frequency cases (250 GHz) also show a 3-dB frequency bandwidth of ±9%.

Figure 8 shows a spectrum of the RF output made using a tunable, narrow-band (75-MHz) YIG filter. The input signal frequency is 36 GHz, with the amplified pulse width of about 7 ns because of the narrow electron beam pulse. The measured line width from Fig. 8 is about 200 MHz, corresponding closely to the Fourier-transform width of the output signal.

To compare the beam energy loss to the RF power gain and to study the effect of the FEL interaction on the electron beam energy spectrum, we use the experimental setup shown in Fig. 9. A spectrograph uses a fast-gated camera to look at the light produced by the magnetically dispersed electrons from the wiggler as they impinge on a fast-response phosphor.[11] The RF power can be measured simultaneously with the electron beam spectrum. The electron spectrograph has an energy resolution of 2%.

Figure 10 shows the electron beam spectrum for cases where the wiggler is off, near, and at resonance. The traces shown are densitometer plots of the phosphor image, with fiducial markers included for calibration. Off-resonance, the measured beam energy is 3.6 MeV, with a FWHM energy spread of <3%. As the wiggler field approaches that required for FEL resonance (3.7 kG), the beam energy distribution broadens, with the average beam energy significantly reduced. At resonance, the average beam energy is about 3.2 MeV, corresponding to a 12% energy loss. The total RF power measured for this case is

250 MW, corresponding to 8.6% of the beam energy (2.9 GW) and comparing well with the energy loss measurement.

Detailed measurements at 35 GHz have been reported elsewhere.[2,12,13] These have included measurements of higher-order modes, harmonics, phase evolution, and parametric studies of gain and saturated power against input power and beam current. Good agreement with the simulation codes was obtained for most measurements.

140-GHZ RESULTS

The experimental configuration used to study the operation of ELF at 140 GHz is shown in Fig. 11. No major changes were required in the accelerator or wiggler, except for operating at a lower wiggler field to satisfy the synchronism condition in Eq. (1).

In order to operate at a significantly higher frequency, several changes were required in the microwave beamline. The microwave source is a commercial Extended Interaction Oscillator (EIO) tube producing about 250 W over a 5-μs pulse. A high-voltage vacuum tube power supply and modulator, regulated to 0.5%, provide frequency stability and tube protection. A high-power isolator, rated at 200-W peak, is used at the output of the EIO to minimize the effect of any reflected power.

Based on results of code simulations, we require a minimum of 10 W of RF power into the wiggler to obtain reasonable output signal levels. To ensure minimal and repeatable insertion losses from the EIO to the wiggler, we use a quasi-optical (Q-O) section to inject the signal from a fundamental WR- waveguide into the 3 x 10-cm wiggler waveguide. This consists of a teflon lens to collimate the diffracting microwave signal into a parallel wavefront

at the oversized waveguide. A 90-lpi mesh reflects the RF signal into the wiggler. Insertion loss measurements indicate that about 30 W couple into the wiggler, with a power density on axis that corresponds to about 50 W because of a slight focusing of the signal beam from the lens.

The oversized waveguide continues from the end of the wiggler to the diffraction loss chamber to minimize tapers and joints that may cause mode conversion or high-power reflections back to the EIO. Power is received by an open-ended WR-8 waveguide that is also used as an oversized waveguide to propagate the signal outside the vault to crystal detectors. Because of lack of available low-pass and bandpass filters, only limited spectral measurements are possible using bandpass filters at specific frequencies of 140 and 94 GHz. Calibration is done in a manner similar to that described for the 35-GHz experiments, using a 50-mW IMPATT source and thermocouple power meter for low-power measurements and the EIO pulse for a second, single-pass measurement.

Figure 12 presents a detuning curve from a FRED simulation. It indicates an 11% shift in the detuning curve from (on-axis) FEL synchronism, caused by space-charge and emittance effects. The on-axis field corresponding to FEL synchronism is 1.87 kG, while the peak of the detuning curve is at 1.66 kG. For 35 GHz, this shift from synchronism was significantly less (about 5%). As Fig. 12 indicates, only about half of the output power is calculated to be in the TE_{01} mode for a flat wiggler.

Figure 13 shows a detuning curve measured at 138 GHz for a 4.0-m uniform wiggler. The peak of the detuning curve is at about 1.76 kG, in agreement with the shift calculated above with FRED. The shape and width of the measured curve are in reasonable agreement with the simulations, although there is some asymmetry in the experimental data. The asymmetry may be due to

a peak in the measured gain curve that is about 2% below that calculated with FRED (as observed at 35 GHz), or due to contributions from higher-order modes. The latter is possible because, at 140 GHz, the receiving antenna is marginally in the near-field of the radiation field and can be expected to pick up some of the TE_{21} mode. The apparent baseline slope in the experimental data results from spontaneous emission (discussed below).

Figure 14 shows a gain curve measured at 140 GHz, along with simulation results. Both show a gain of about 20 dB/m and a peak power of about 100 MW. The output power saturates at a length of 3.4 m, in good agreement with simulation results, and begins to decrease as expected because of the synchrotron motion of beam electrons. Simulations predict a synchrotron period of 1.8 m.

Because the signal saturates, we can attempt to increase power by empirically tapering the wiggler. Only three wiggler-control segments (six periods) can be used because of the relatively long exponential-growth region. As shown in Fig. 15, no significant increase in power is achieved using the usual tapering procedure.[10] This result is observed in a simulation of the experiment, which is also plotted in Fig. 15, and shows good agreement with the measured gain profile. Extensive simulations have shown that, for the experimental conditions available (in particular, the maximum wiggler length and input power), tapering by a simple reduction in wiggler field will not significantly increase the FEL efficiency.

One contribution to the reduction in tapering efficiency arises from the large shift in the gain curve away from FEL synchronism, as seen in Fig. 12. The relative FEL power gain caused by tapering is given by:

$$\frac{\Delta P_s}{P_s} = F_T \left(\frac{\Delta\gamma}{\gamma}\right) \quad , \tag{4}$$

where P_s is the signal power, F_T is the trapped fraction of beam electrons, and $\Delta\gamma$ is the loss in beam energy caused by tapering.

Maximum gain of the injected signal, and minimum growth of spontaneous noise, occur at the peak of the detuning curve. Effective trapping of the electrons requires that the beam be close to synchronism (Eq. 1). When the peak of the detuning curve is shifted well away from synchronism by space-charge effects--as it is for the 140-GHz experiments at 3.5 MeV--the initial trapping (near the end of the exponential gain regime) is greatly reduced, and further detrapping occurs as one attempts to taper.

A higher beam energy (and corresponding wiggler field) would result in reduced space-charge effects,[8] and hence a more effective taper. Simulation studies have shown, however, that a tapering procedure also exists that can improve tapered wiggler performance despite space-charge effects. Figure 16 shows a tapering profile and the corresponding gain profile for a simulation in which the wiggler field is chosen to maximize exponential gain. At a point near saturation, the wiggler field is increased to bring the signal wave and electron beam bunches into synchronism before tapering occurs. The gain profile shows a factor-of-four improvement in output power for this taper, but also indicates that a longer wiggler length would have been required to observe this effect.

Thus, simulations appear to model the gain profile well, even for tapered-field profiles that are not optimal. Simulation studies indicate that space-charge effects are significant for the conditions of the experiment, and have suggested a tapering procedure that could help mitigate these effects.

As noted in the discussion of Fig. 13, there is a significant level of spontaneous noise away from the peak of the detuning curve that is independent

of the EIO source. Figure 17 shows two waveforms of the output signal made with and without an input signal. For the 30-W input signal used in these experiments, the spontaneous noise level is approximately 15 dB below the driven level. The traces shown were taken for a short beam pulse, but illustrate the difference in pulse shape and pulse-to-pulse repeatability for the two cases. The driven case on the left shows an RF pulse that is relatively flat and at high powers varies about 20% shot to shot. The spontaneous signal on the right, however, is observed to vary strongly both during the pulse and from pulse to pulse, indicating a wide frequency bandwidth and random phases. Measurements of the driven output RF spectrum, using an F-band wavemeter (300-MHz resolution), are consistent with a transform-limited bandwidth, as observed at 35 GHz. The spontaneous bandwidth, as inferred from the detuning curve, would span a broad frequency range of about 10%.

Figure 18 shows a detuning curve made over a wide range of wiggler magnetic field settings and without any filtering of the signal. Each wiggler field setting corresponds to a different frequency for FEL resonance; several frequencies that correspond to a 15% reduction in the wiggler field from that given by Eq. (1)--because of effects not included in that approximate expression--are indicated on Fig. 18. The driven signal at 140 GHz (1.7 kG) is correlated with the presence of the input signal, while the rest of the "spectrum" is not affected by the input drive. Bandpass measurements of the spectrum at 140 and 94 GHz show that the frequency of the spontaneous signal in each field setting indeed corresponds to expected FEL resonance. Signal levels could be calibrated at only 94 and 140 GHz, as indicated, so that details of the shape of the spectrum cannot be inferred from Fig. 18. The signal decrease for fields above 2.6 kG corresponds to the cutoff frequency of the WR- waveguide (74 GHz).

Figure 19 shows a GINGER simulation of the growth of spontaneous emission (shot noise) at a wiggler field corresponding to peak gain at 94 GHz. An exponential gain of 28 dB/m is calculated, with an overall gain of 105 dB for the 3.72-m length and a spectral width of about 10%. Similar simulations for 140 GHz predict an exponential gain of 21 dB/m and an overall gain of 85 dB.

Figure 20 shows a gain curve measured at 2.4 kG with both the unfiltered channel and the 94-GHz bandpass-filtered channel. The reduced power measured for the filtered channel results primarily from the narrow bandpass (3%) of the 94-GHz filter, in contrast to the broadband spectrum measured for the unfiltered signal. Exponential gains of 25-27 dB/m and overall gains of 88-95 dB are measured, in reasonable agreement with the simulations. The signals are observed to saturate at output power levels that correspond to an effective input power of 70 mW. Similarly, the driven- and spontaneous-signal levels measured at 140 GHz imply an effective input power of 10-100 mW, also about 20 dB above that expected from shot noise.

Thus, the spontaneous emission measurements are in reasonable agreement with the code simulations if one takes the effective input signal as 15-25 dB above shot noise. If one accounts for the spectral bandwidth of the measurements, the input spectral power density is 1-50 mW/GHz. Previous superradiant measurements on ELF at 35 GHz[12] indicated an effective input signal of 1.5 mW (about 1 mW/GHz). Shot noise represents only a theoretical lower limit to the noise, so that the larger effective input noise is not implausible. The measured noise values represent a basis upon which to calculate the required input power of a master oscillator for microwave FEL amplifiers.

CONCLUSIONS

ELF is capable of producing very high gain and intense microwave radiation at both 35 and 140 GHz. The experimental characteristics of ELF at 35 and 140 GHz show good agreement with particle simulation codes in both the linear and nonlinear regimes. For identical electron beam conditions, the gain, output power, and efficiency are reduced at 140 GHz.

Only relatively minor changes in the experimental facility were required to achieve this wide range, suggesting that this FEL configuration is a useful form of tunable, pulsed, high-power radiation in the millimeter region.

ACKNOWLEDGMENTS

We would like to thank the ETA staff, led by J. Crawford and S. Hawley, for their valuable contribution in operating the ETA facility. In particular, we thank S. Fields and J. Johnson for the design and fabrication of the EIO power supply; J. Dunlap for the calibration and testing of the microwave subsystems; N. Liggins, B. Rego, and C. Holmes for the fabrication of mechanical components; and D. Rogers for his coordination efforts. C. Parkison and B. Pedrotti designed and fabricated much of the 2-mm waveguide components. We are also pleased to acknowledge the participation of Mr. S. Evangelides and Dr. K. E. Kreischer of the MIT Plasma Fusion Center in spectral measurements of the 140-GHz radiation.

Table 1. Operating parameters for FEL experiments at 35 and 140 GHz

ETA beam:	• 3.5 MeV (γ = 7.8) • 800-1000 A through wiggler • Brightness = 2 x 10^4 A/(cm-rad)^2 • Pulse length = 10-15 ns
ELF wiggler:	• Wiggler wavelength = 9.8 cm • L_w = 3.0 → 4.0 m • f = 35 GHz (140 GHz) • B_w = 3.7 kG (1.7 kG) • a_w = 2.4 (1.1) • P_{in} = 50 kW (30 W)
FEL output:	• P_{out} = 1.0 GW, tapered (50 MW, untapered) • Conversion efficiency = 35% (2%)

REFERENCES

1. T. J. Orzechowski et al., "Microwave Radiation from a High-Gain Free-Electron Laser Amplifier," Phys. Rev. Lett. 54, (1985), 889.

2. D. B. Hopkins et al., "High-power 35 GHz testing of a free-electron laser and two-beam accelerator structures," Proc. of SPIE Conf. on High-Intensity Laser Processes 664 (1986), 61.

3. W. M. Nevins, T. D. Rognlien, B. I. Cohen, Nonlinear Limits on Electron Heating with Intense Microwave Pulses, Lawrence Livermore National Laboratory, Livermore, Calif., UCRL-59006 (1986). Submitted to Phys. Rev. Lett.

4. R. E. Hester et al., "The Experimental Test Accelerator (ETA)," IEEE Trans. Nucl. Sci. NS-26 (1979), 3.

5. E. T. Scharlemann, J. Appl. Phys. 58 (1985), 2154.

6. W. M. Fawley, D. Prosnitz, E. T. Scharlemann, Phys. Rev. A30 (1984), 2472.

7. N. M. Kroll, P. L. Morton, M. R. Rosenbluth, IEEE J. Quantum Electron. QE-17 (1981), 1436.

8. T. C. Marshall, Free-Electron Lasers (MacMillan Publishing Co, New York, 1985).

9. D. Prosnitz, A. Szoke, and V. K. Neil, Phys. Rev. A 24 (1981), 1436.

10. T. J. Orzechowski et al., "High-efficiency extraction of microwave radiation from a tapered-wiggler free-electron laser," Phys. Rev. Lett. 57 (1986), 2172.

11. B. Kulke, M. J. Burns, T. J. Orzechowski, A Wideband Spectrograph for Free Electron Laser Experiments, Lawrence Livermore National Laboratory, Livermore, Calif., UCRL-95598. To be published in Rev. Sci. Instrum. (1987).

12. T. J. Orzechowski et al., "High-gain and high extraction efficiency from a free electron laser amplifier operating in the millimeter wave regime," Nucl. Instrum. Meth. Phys. Res. A 250 (1986), 144.

13. T. J. Orzechowski, E. T. Scharlemann, and D. B. Hopkins, "Measurement of the phase of the electromagnetic wave in a free-electron laser amplifier," Phys. Rev. A 35 (1987), 2184.

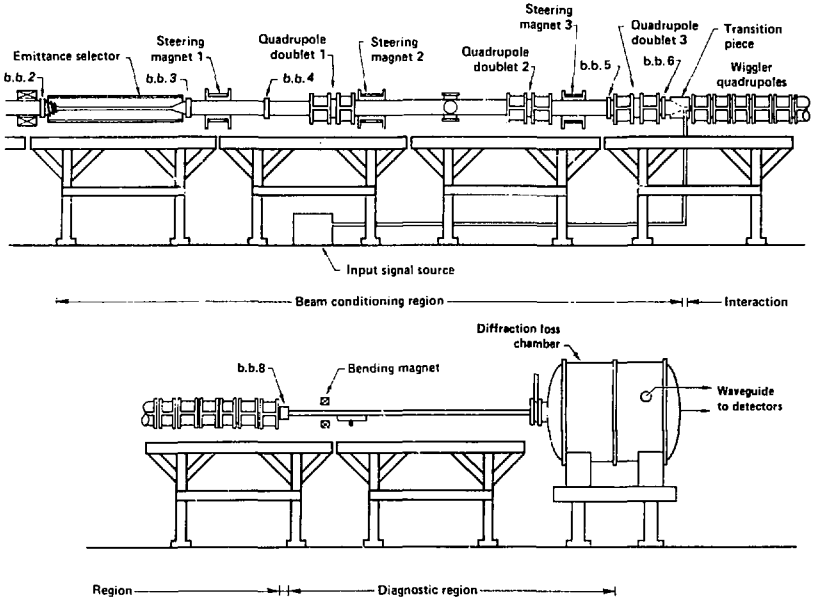

Fig. 1 Layout of major ELF components.

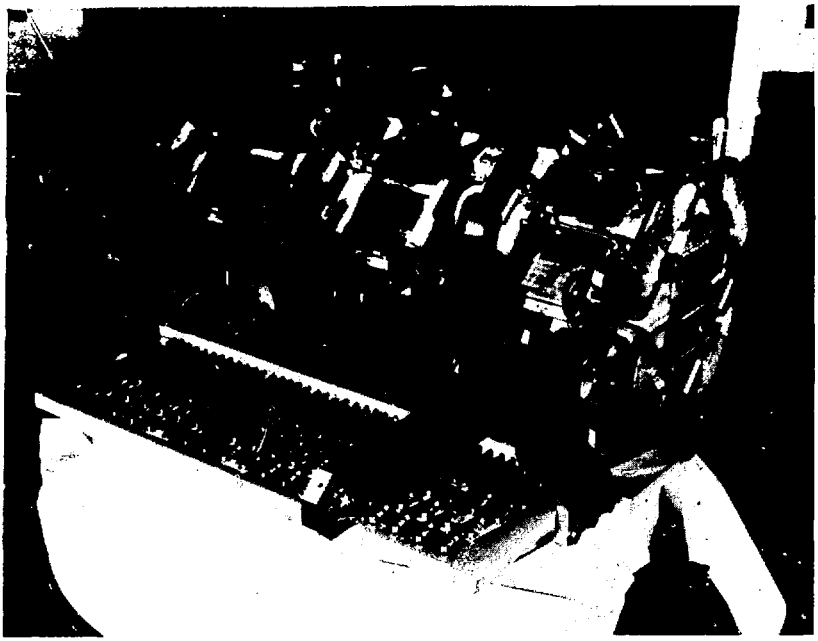

Fig. 2 1-m section of ELF wiggler.

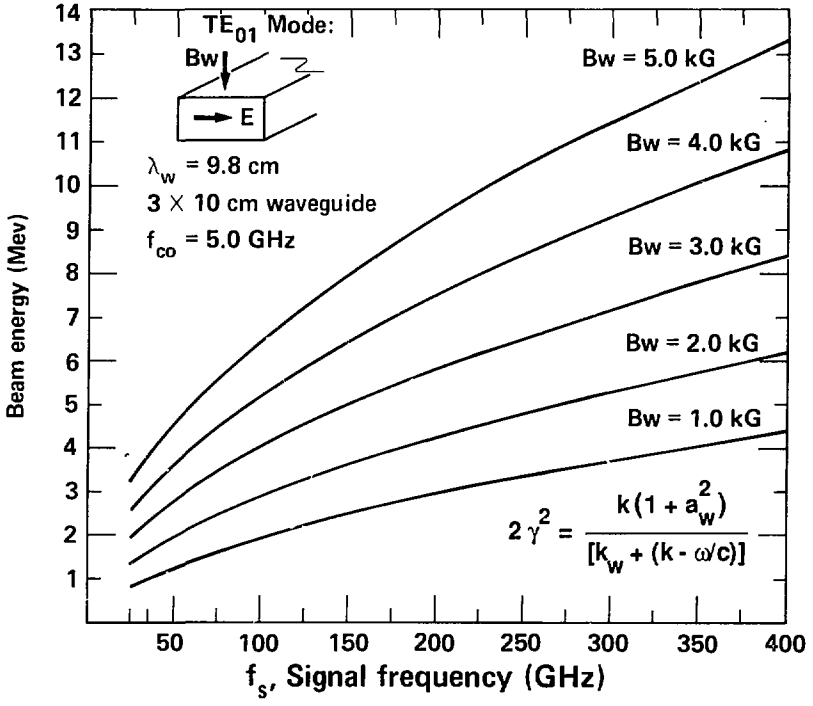

Fig. 3 Resonance condition for waveguided FEL for a range of operating parameters.

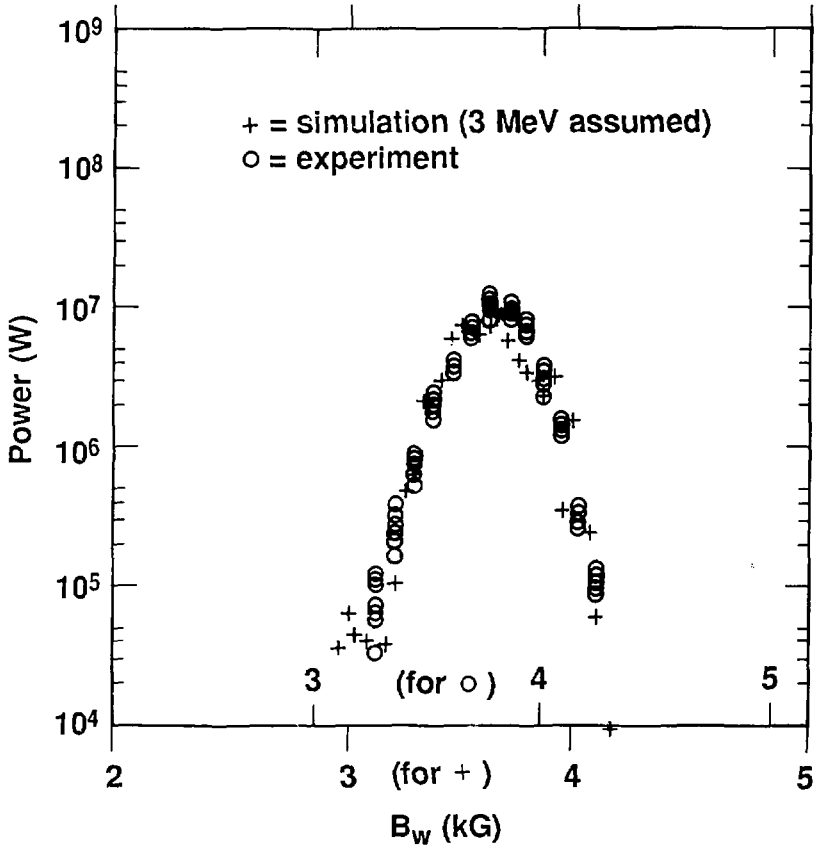

Fig. 4 Detuning curve for 1-m wiggler length.

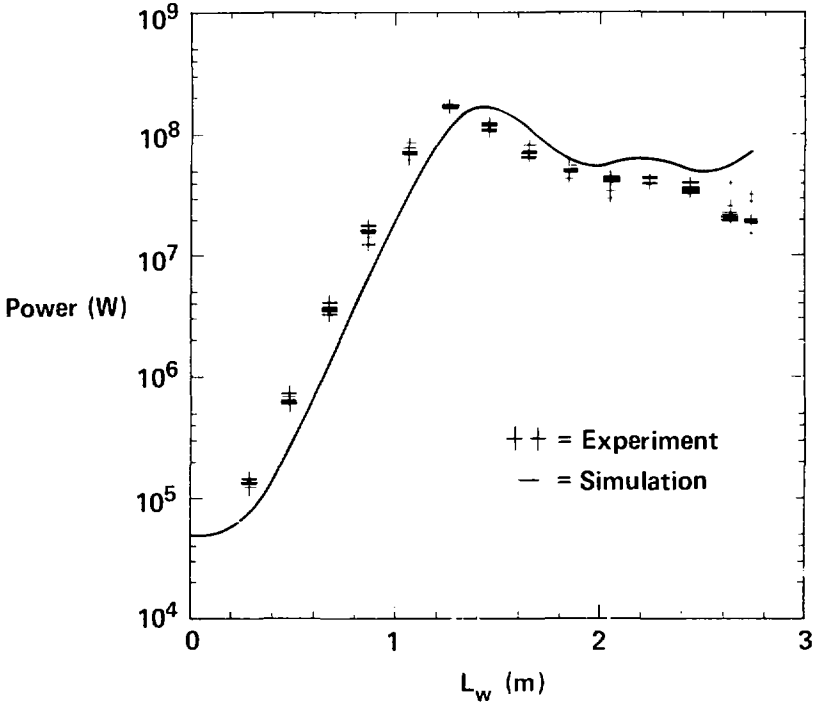

Fig. 5 35-GHz gain curve for a uniform wiggler field.

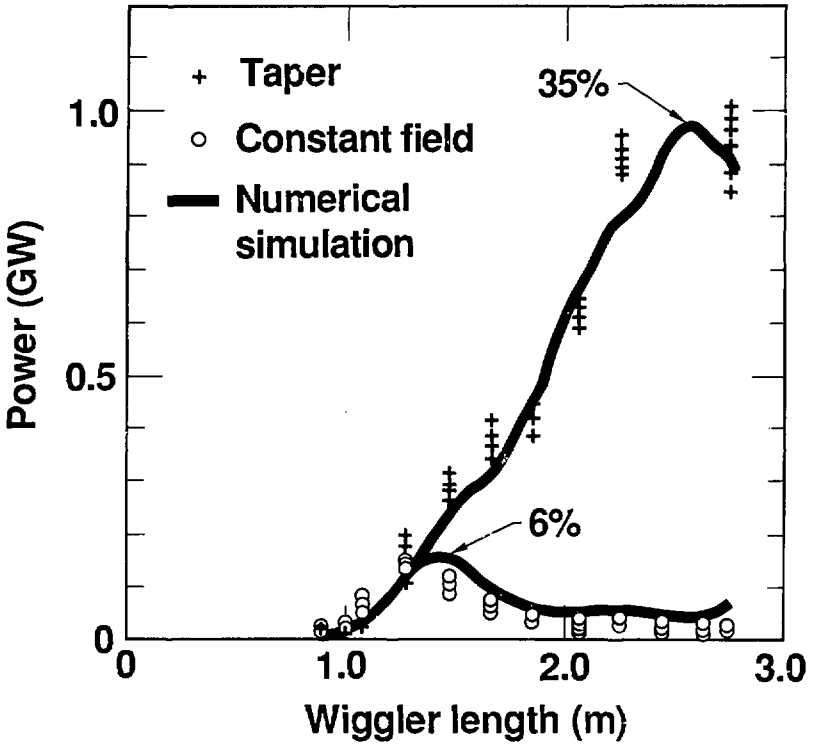

Fig. 6 Gain curve comparison for uniform and tapered wiggler.

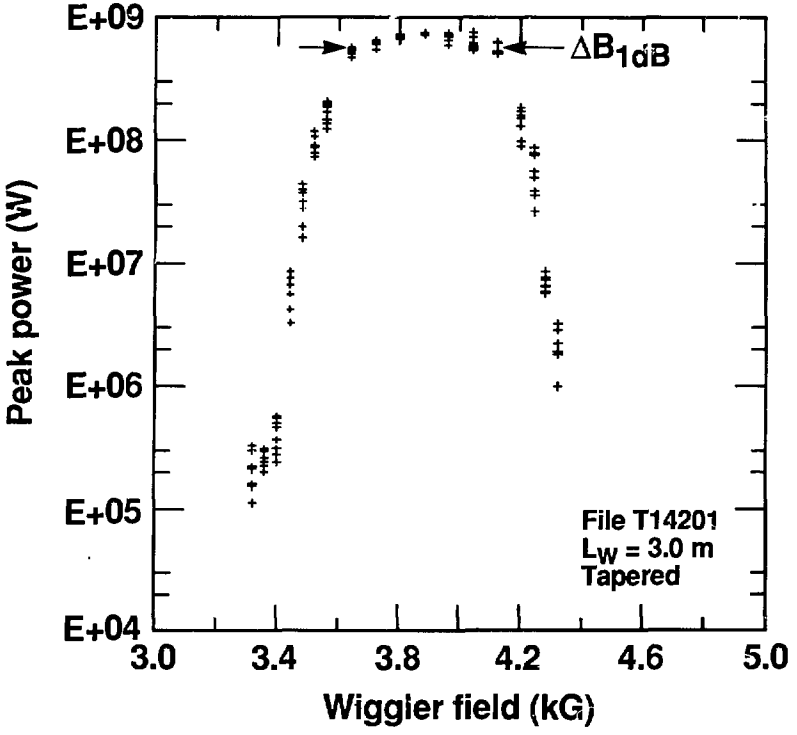

Fig. 7 Detuning curve at 35 GHz for a tapered wiggler.

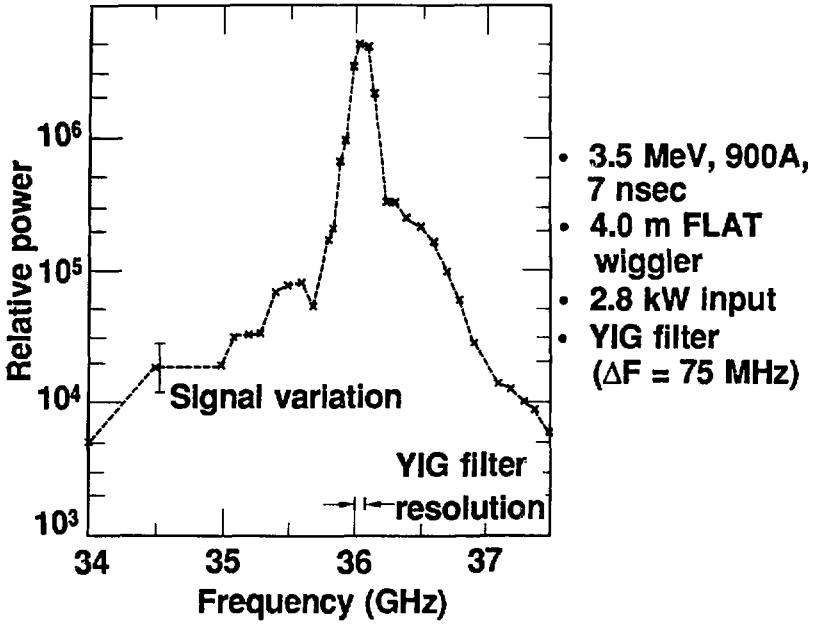

Fig. 8 Output spectrum of a 36 GHz signal.

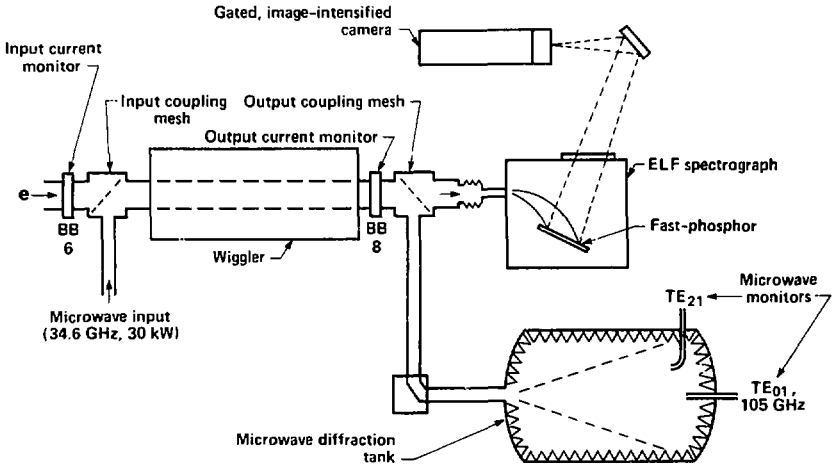

Fig. 9 Experiment to measure e-beam energy spectrum.

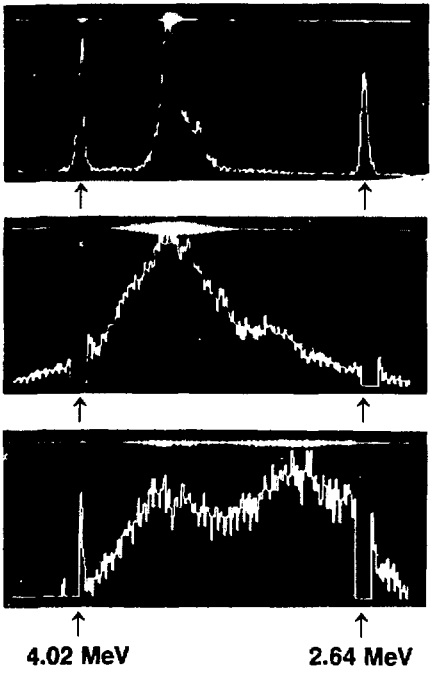

Fig. 10 E-beam spectrum for different wiggler field settings.

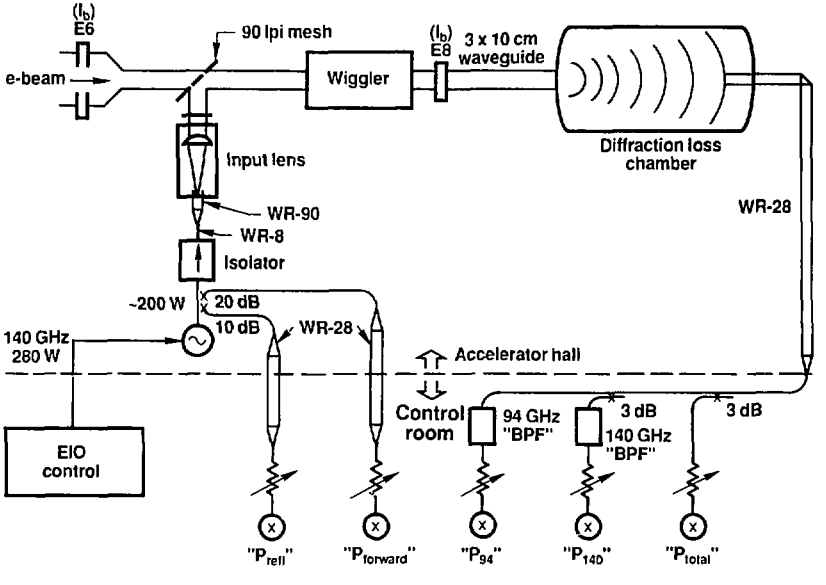

Fig. 11 Configuration of ELF 140-GHz experiment.

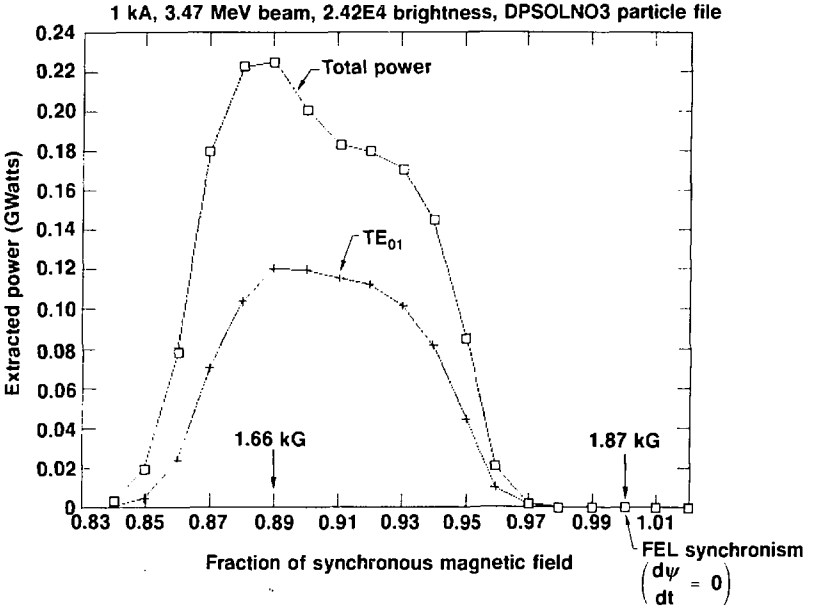

Fig. 12 Detuning curve for 140 GHz as predicted by simulations.

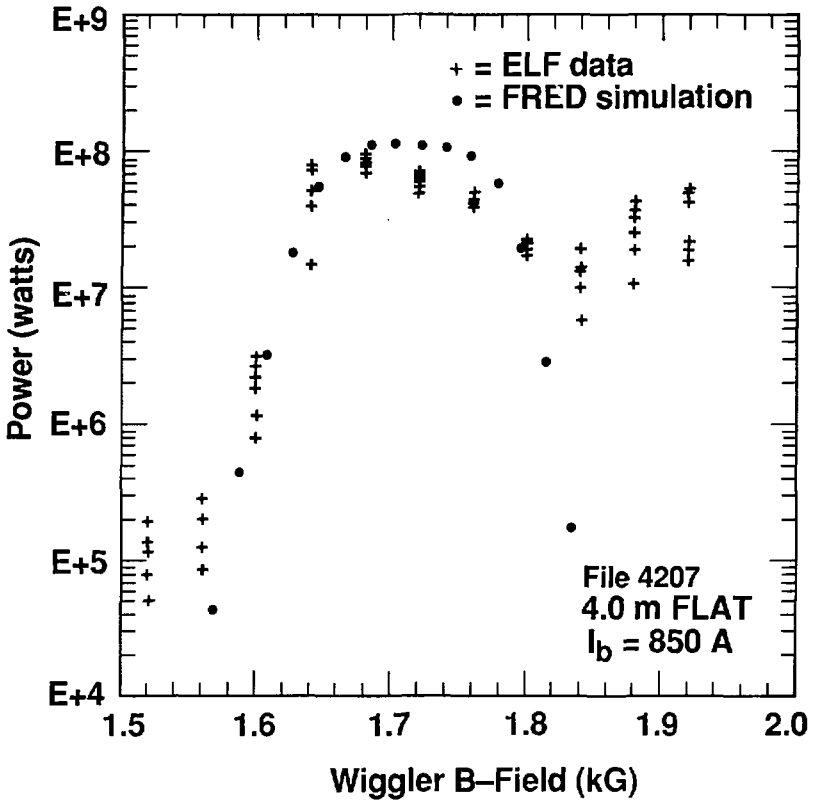

Fig. 13 Detuning curves for 140-GHz signal as measured and predicted by simulations.

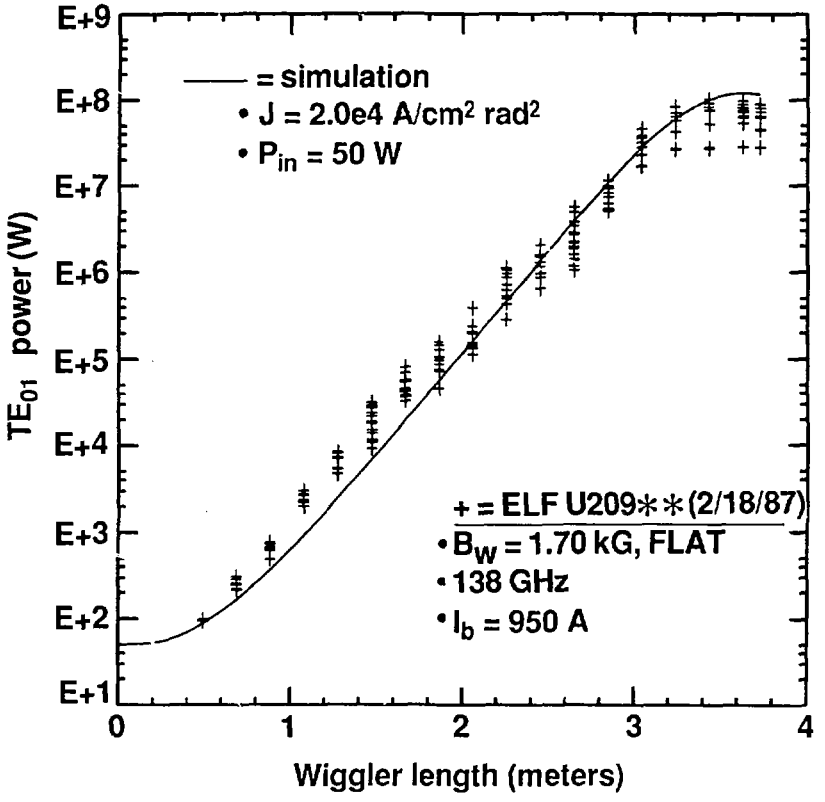

Fig. 14 Gain curve at 140 GHz as measured and predicted by simulations for a FLAT wiggler.

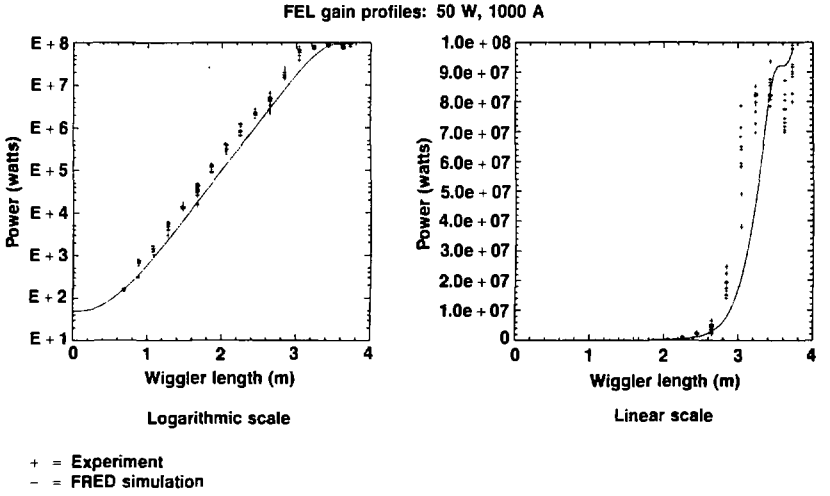

Fig. 15 Measured and simulated gain curves at 140 GHz for an empirically tapered wiggler.

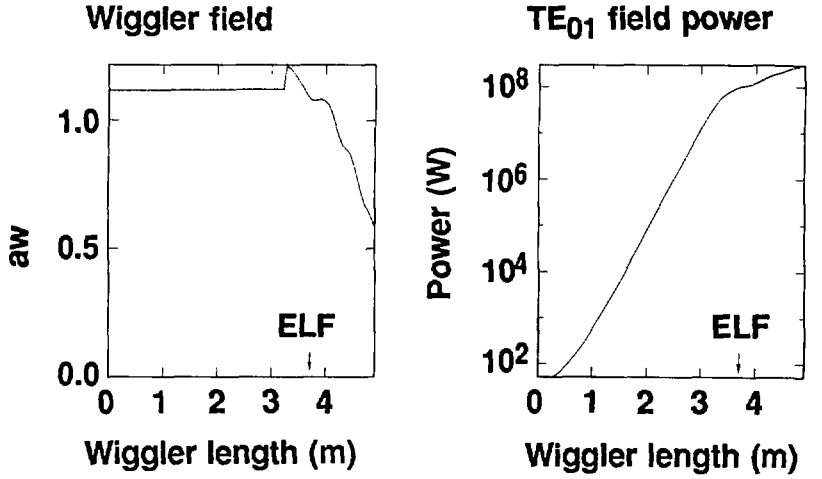

Fig. 16 Simulation of optimized taper at 140 GHz and 3.5 MeV.

Fig. 17 RF output signals with (left) and without (right) input signal.

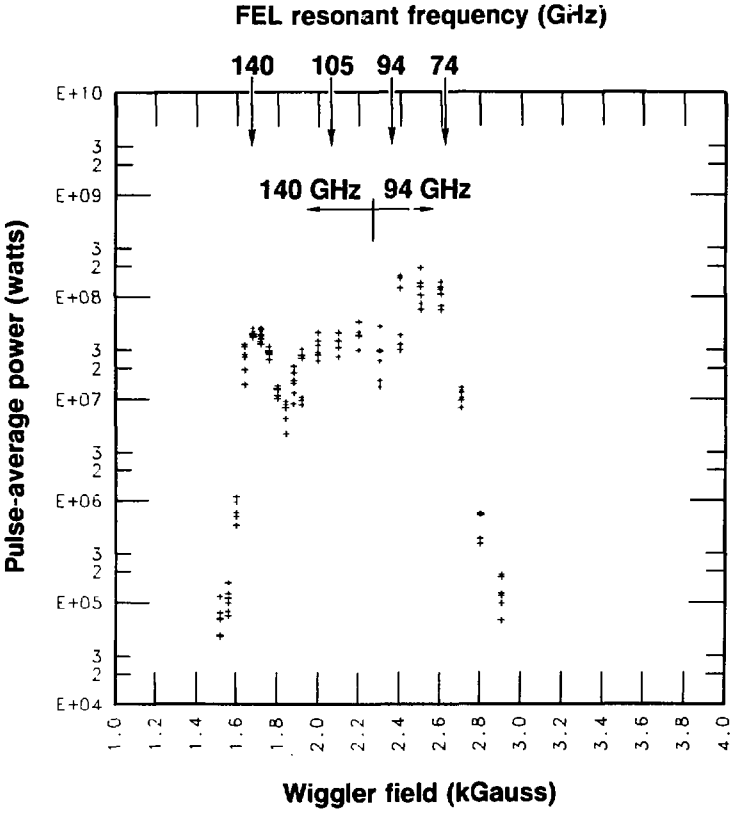

Fig. 18 Broadband emission from ELF as measured over a range of wiggler field strengths.

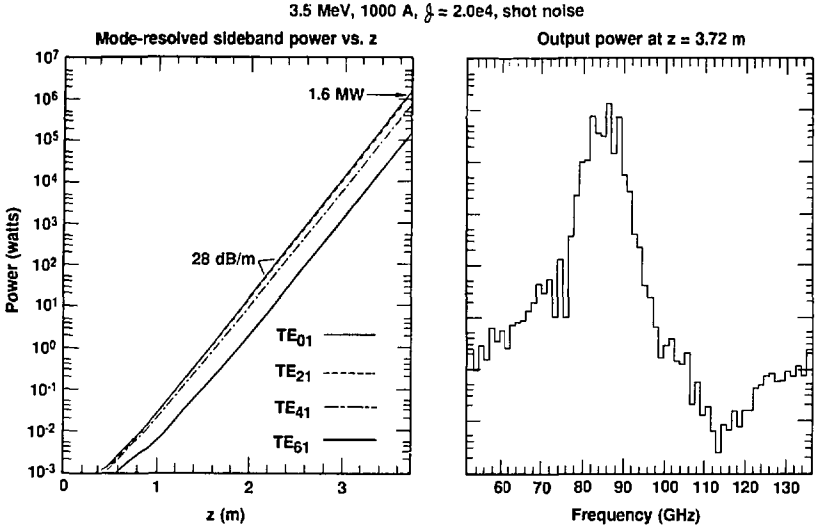

Fig. 19 Simulation of broadband growth from shot noise for 2.4-kG wiggler field.

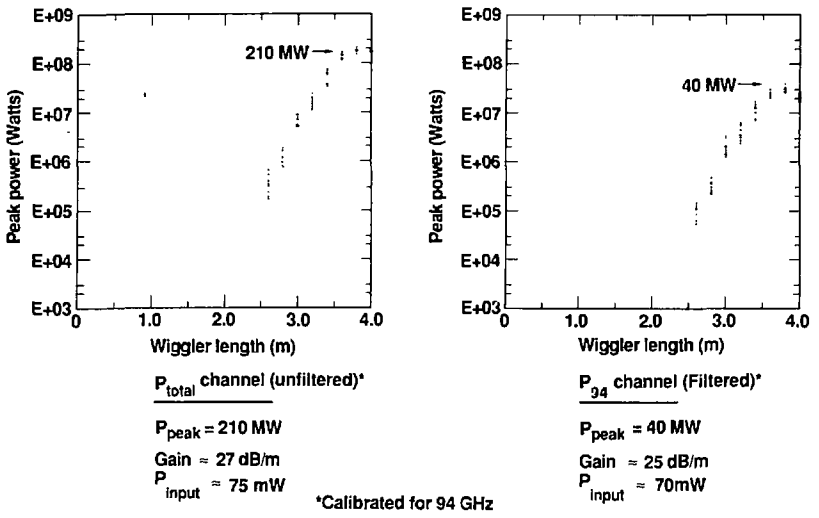

Fig. 20 Gain curve of spontaneous emission measured at 2.4 kG, with and without a BPF.